

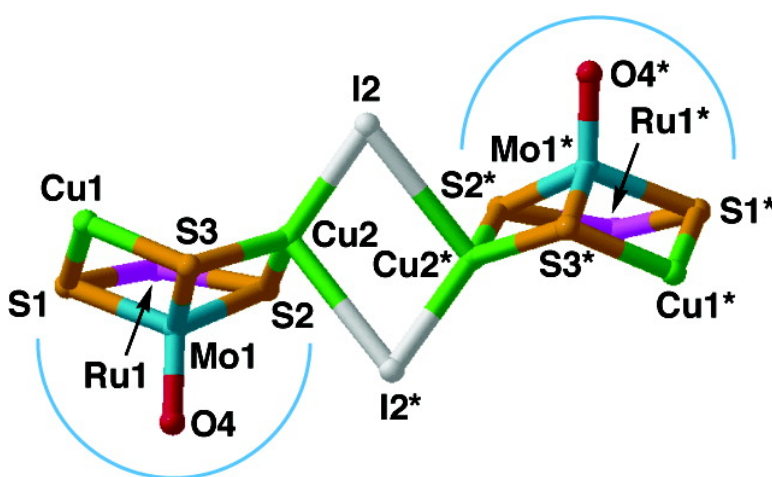
Article

Synthesis and Crystal Structure of an Open Capsule-Type Octanuclear Heterometallic Sulfide Cluster with a Linked Incomplete Double Cubane Framework without an Intramolecular Inversion Center

Bunsho Kure, Seiji Ogo, Daisuke Inoki, Hidetaka Nakai, Kiyoshi Isobe, and Shunichi Fukuzumi

J. Am. Chem. Soc., 2005, 127 (41), 14366-14374 • DOI: 10.1021/ja051748q • Publication Date (Web): 27 September 2005

Downloaded from <http://pubs.acs.org> on March 25, 2009



More About This Article

Additional resources and features associated with this article are available within the HTML version:

- Supporting Information
- Access to high resolution figures
- Links to articles and content related to this article
- Copyright permission to reproduce figures and/or text from this article

[View the Full Text HTML](#)

Synthesis and Crystal Structure of an Open Capsule-Type Octanuclear Heterometallic Sulfide Cluster with a Linked Incomplete Double Cubane Framework without an Intramolecular Inversion Center

Bunsho Kure,[†] Seiji Ogo,^{*,†} Daisuke Inoki,[†] Hidetaka Nakai,[‡] Kiyoshi Isobe,[‡] and Shunichi Fukuzumi^{*,†}

Contribution from the Department of Material and Life Science, Graduate School of Engineering, Osaka University, PRESTO and SORST, Japan Science and Technology Agency (JST), Suita, Osaka 565-0871, Japan, and Department of Chemistry, Faculty of Science, Kanazawa University, Kakuma-machi, Kanazawa 920-1192, Japan

Received March 18, 2005; Revised Manuscript Received August 24, 2005; E-mail: ogo@ap.chem.eng.osaka-u.ac.jp

Abstract: An open capsule-type octanuclear heterometallic sulfide cluster without an intramolecular inversion center $[\text{Ru}(\eta^6\text{-C}_6\text{Me}_6)\{\text{P}(\text{OMe})_3\}\{\text{MoO}(\mu_3\text{-S})_3\}(\text{CuI})_2]_2$ (**5**) has been synthesized for the first time by stepwise connection of three mononuclear building blocks, i.e., (i) $[\text{RuCl}_2(\eta^6\text{-C}_6\text{Me}_6)\{\text{P}(\text{OMe})_3\}]$ (**1a**) as an octahedral terminal building block to control the direction of cluster expansion, (ii) $[\text{MoOS}_3]^{2-}$ as a tetrahedral polydentate building block owing to the strong coordination ability of the S atoms, and (iii) a CuI building block to form a trigonal planar $(\mu\text{-S})_2\text{CuI}$ unit or to form a linkage unit of two incomplete cubane-type octanuclear frameworks. The stepwise connection was made in the following order: $[\text{RuCl}_2(\eta^6\text{-C}_6\text{Me}_6)\{\text{P}(\text{OMe})_3\}]$ (**1a**, mononuclear) \rightarrow $[\text{Ru}(\eta^6\text{-C}_6\text{Me}_6)\{\text{P}(\text{OMe})_3\}\{\text{MoOS}(\mu_2\text{-S})_2\}]$ (**2a**, dinuclear) \rightarrow $[\text{Ru}(\eta^6\text{-C}_6\text{Me}_6)\{\text{P}(\text{OMe})_3\}\{\text{MoO}(\mu_2\text{-S})_2(\mu_3\text{-S})\}\text{CuI}]$ (**3a**, butterfly-type trinuclear) \rightarrow $[\text{Ru}(\eta^6\text{-C}_6\text{Me}_6)\{\text{P}(\text{OMe})_3\}\{\text{MoO}(\mu_3\text{-S})_3\}(\text{CuI})_2]_2$ (**5**). When $\text{P}(\text{OMe})_3$ was replaced by $\text{P}(\text{OEt})_3$, which is more bulky than $\text{P}(\text{OMe})_3$, in the starting ruthenium building block $[\text{RuCl}_2(\eta^6\text{-C}_6\text{Me}_6)\{\text{P}(\text{OEt})_3\}]$ (**1b**, mononuclear), only the tetranuclear incomplete single cubane cluster $[\text{Ru}(\eta^6\text{-C}_6\text{Me}_6)\{\text{P}(\text{OEt})_3\}\{\text{MoO}(\mu_3\text{-S})_3\}(\text{CuI})_2]$ (**6**) was generated, owing to the steric effect of $\text{P}(\text{OEt})_3$.

Introduction

Extensive efforts have so far been devoted to synthesize metal sulfide and oxide clusters with complete cubane or incomplete cubane frameworks because of the interest in their geometrical relevance to the active site structures of enzymes with cubane-like units such as Fe_4S_4 and Mn_4O_4 as well as potential applications in the area of catalysis.^{1–9}

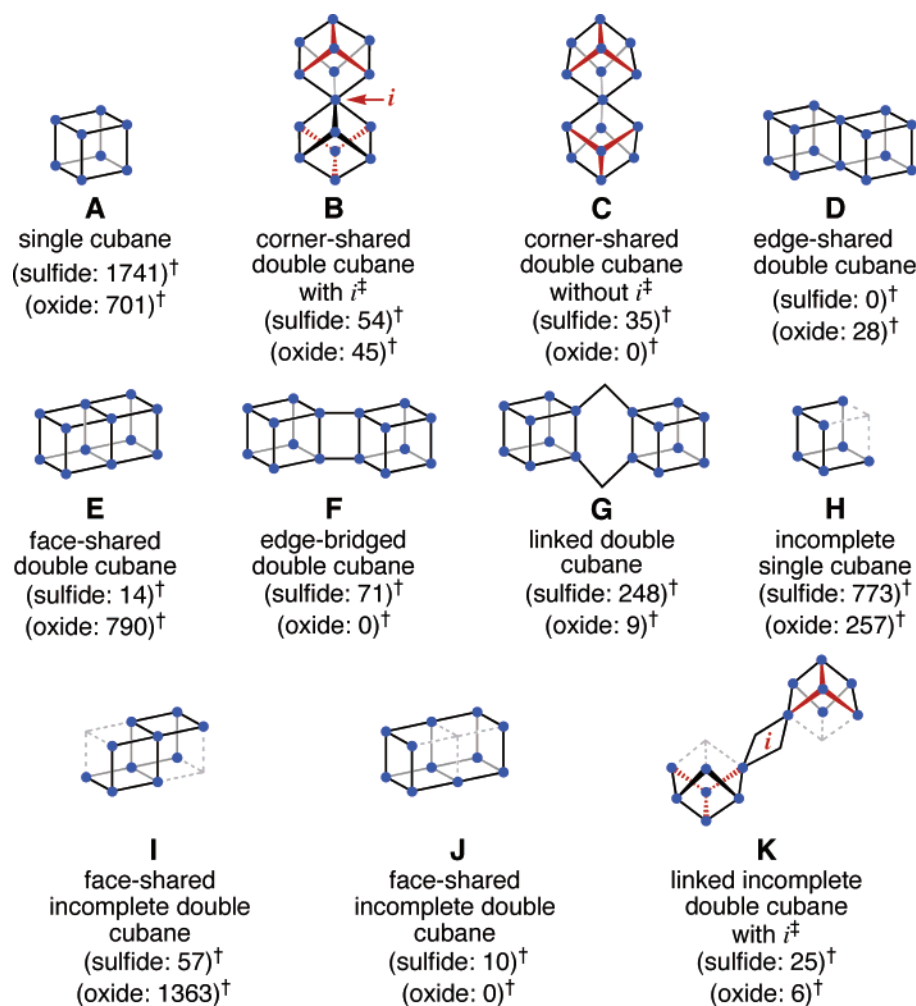
Chart 1 shows different types of metal sulfide and oxide clusters so far synthesized with complete cubane frameworks {e.g., **A**, single cubane;^{10,11} **B**, corner-shared double cubane with an intramolecular inversion center (*i*);^{12–14} **C**, corner-shared

[†] Osaka University, PRESTO and SORST, JST.

[‡] Kanazawa University.

- (1) (a) Rao, P. V.; Holm, R. H. *Chem. Rev.* **2004**, *104*, 527–559. (b) Lee, S. C.; Holm, R. H. *Chem. Rev.* **2004**, *104*, 1135–1157. (c) Holm, R. H. *Adv. Inorg. Chem.* **1992**, *38*, 1–71.
- (2) (a) Shibahara, T. *Coord. Chem. Rev.* **1993**, *123*, 73–147. (b) Shibahara, T. *Adv. Inorg. Chem.* **1991**, *37*, 143–173.
- (3) Coucouvanis, D. *Acc. Chem. Res.* **1991**, *24*, 1–8.
- (4) Harris, S. *Polyhedron* **1989**, *8*, 2843–2882.
- (5) (a) Hernandez-Molina, R.; Sokolov, M. N.; Sykes, A. G. *Acc. Chem. Res.* **2001**, *34*, 223–230. (b) Hernández-Molina, R.; Sykes, A. G. *J. Chem. Soc., Dalton Trans.* **1999**, 3137–3148. (c) Hernandez-Molina, R.; Sykes, A. G. *Coord. Chem. Rev.* **1999**, *187*, 291–302.
- (6) (a) Llusar, R.; Uriel, S. *Eur. J. Inorg. Chem.* **2003**, 1271–1290. (b) Ama, T.; Rashid, M. M.; Yonemura, T.; Kawaguchi, H.; Yasui, T. *Coord. Chem. Rev.* **2000**, *198*, 101–116. (c) Hidai, M.; Kuwata, S.; Mizobe, Y. *Acc. Chem. Res.* **2000**, *33*, 46–52. (d) Ogino, H.; Inomata, S.; Tobita, H. *Chem. Rev.* **1998**, *98*, 2093–2121. (e) Bayón, J. C.; Claver, C.; Masdeu-Bultó, A. M. *Coord. Chem. Rev.* **1999**, *193–195*, 73–145. (f) Hou, H.-W.; Xin, X.-Q.; Shi, S. *Coord. Chem. Rev.* **1996**, *153*, 25–56. (g) Isobe, K.; Yagasaki, A. *Acc. Chem. Res.* **1993**, *26*, 524–529.
- (7) (a) Seino, H.; Masumori, T.; Hidai, M.; Mizobe, Y. *Organometallics* **2003**, *22*, 3424–3431. (b) Takei, I.; Wakebe, Y.; Suzuki, K.; Enta, Y.; Suzuki, T.; Mizobe, Y.; Hidai, M. *Organometallics* **2003**, *22*, 4639–4641. (c) Murata, T.; Mizobe, Y.; Gao, H.; Ishii, Y.; Wakabayashi, T.; Nakano, F.; Tanase, T.; Yano, S.; Hidai, M.; Echizen, I.; Nanikawa, H.; Motomura, S. *J. Am. Chem. Soc.* **1994**, *116*, 3389–3398.
- (8) (a) Demadis, K. D.; Coucouvanis, D. *Inorg. Chem.* **1995**, *34*, 3658–3666. (b) Malinak, S. M.; Demadis, K. D.; Coucouvanis, D. *J. Am. Chem. Soc.* **1995**, *117*, 3126–3133. (c) Demadis, K. D.; Coucouvanis, D. *Inorg. Chem.* **1994**, *33*, 4195–4197.
- (9) (a) Yamamura, T.; Christou, G.; Holm, R. H. *Inorg. Chem.* **1983**, *22*, 939–949. (b) Tanaka, K.; Hozumi, Y.; Tanaka, T. *Chem. Lett.* **1982**, 1203–1206.
- (10) Type **A** $[\text{M}_4\text{S}_4]$: (a) Herbst, K.; Dahlenburg, L.; Brorson, M. *Inorg. Chem.* **2004**, *43*, 3227–3328. (b) Kawaguchi, H.; Yamada, K.; Ohnishi, S.; Tatsumi, K. *J. Am. Chem. Soc.* **1997**, *119*, 10871–10872. (c) Shibahara, T.; Kobayashi, S.; Tsuji, N.; Sakane, G.; Fukuhara, M. *Inorg. Chem.* **1997**, *36*, 1702–1706. (d) Curtis, M. D.; Riaz, U.; Curnow, O. J.; Kampf, J. W. *Organometallics* **1995**, *14*, 5337–5343. (e) Müller, A.; Eltzner, W.; Clegg, W.; Sheldrick, G. M. *Angew. Chem., Int. Ed. Engl.* **1982**, *21*, 536–537. (f) Averill, B. A.; Herskovitz, T.; Holm, R. H.; Ibers, J. A. *J. Am. Chem. Soc.* **1973**, *95*, 3523–3534.
- (11) Type **A** $[\text{M}_4\text{S}_3\text{Cl}]$: (a) Jeannin, Y.; Sécheresse, F.; Bernès, S.; Robert, F. *Inorg. Chim. Acta* **1992**, *198–200*, 493–505. (b) Müller, A.; Bögge, H.; Tölle, H.-G.; Jostes, R.; Schimanski, U.; Dartmann, M. *Angew. Chem., Int. Ed. Engl.* **1980**, *19*, 654–655. (c) Müller, A.; Hwang, T. K.; Bögge, H. *Angew. Chem., Int. Ed. Engl.* **1979**, *18*, 628–629.
- (12) Type **B** $[\text{M}_7\text{S}_8]$: (a) Shinozaki, A.; Seino, H.; Hidai, M.; Mizobe, Y. *Organometallics* **2003**, *22*, 4636–4638. (b) Fedin, V. P.; Sokolov, M.; Lamprecht, G. J.; Hernandez-Molina, R.; Seo, M.-S.; Virovets, A. V.; Clegg, W.; Sykes, A. G. *Inorg. Chem.* **2001**, *40*, 6598–6603. (c) Hernandez-Molina, R.; Fedin, V. P.; Sokolov, M. N.; Sellsell, D. M.; Sykes, A. G. *Inorg. Chem.* **1998**, *37*, 4328–4334.
- (13) Type **B** $[\text{M}_7\text{S}_6\text{O}_2]$: Sakane, G.; Yao, Y.-G.; Shibahara, T. *Inorg. Chim. Acta* **1994**, *216*, 13–14.
- (14) Type **B** $[\text{M}_7\text{O}_6\text{Cl}_2]$: Liu, X.; McAllister, J. A.; de Miranda, M. P.; Whitaker, B. J.; Kilner, C. A.; Thornton-Pett, M.; Halcrow, M. A. *Angew. Chem., Int. Ed.* **2002**, *41*, 756–758.

Chart 1



[†] Reported numbers based on the data gathered from ACS, SciFinder.

[‡] An intramolecular inversion center.

●: S, O, or metal ions.

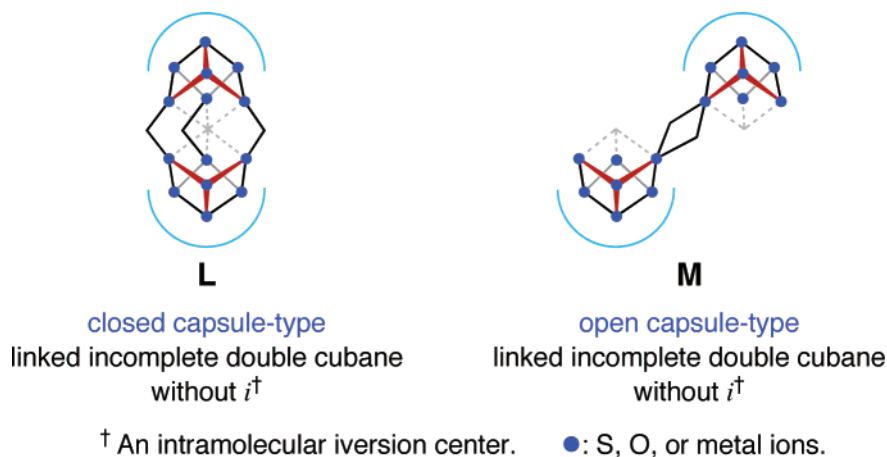
double cubane without i^{\ddagger} ;¹⁵ **D**, edge-shared double cubane;^{16–18} **E**, face-shared double cubane;^{19,20} **F**, edge-bridged double

cubane;²¹ and **G**, linked double cubane²² and incomplete cubane frameworks (e.g., **H**, incomplete single cubane;^{23–25} **I**, face-shared incomplete double cubane;^{26–28} **J**, face-shared incomplete double cubane;^{29,30} and **K**, linked incomplete double cubane with i^{\ddagger}).

- (15) Type C [M_8S_7]: (a) Zhang, Y.; Holm, R. H. *J. Am. Chem. Soc.* **2003**, *125*, 3910–3920. (b) Zuo, J.-L.; Zhou, H.-C.; Holm, R. H. *Inorg. Chem.* **2003**, *42*, 4624–4631. (f) Ohki Y.; Sunada, Y.; Honda, M.; Katada, M.; Tatsumi, K. *J. Am. Chem. Soc.* **2002**, *125*, 4052–4053.
- (16) Type D [M_4O_7]: (a) Hegetschweiler, K.; Finn, R. C.; Rarig, R. S., Jr.; Sander, J.; Steinhäuser, S.; Wörle, M.; Zubieta, J. *Inorg. Chim. Acta* **2002**, *337*, 39–47. (b) Besserguenev, A. V.; Dickman, M. H.; Pope, M. T. *Inorg. Chem.* **2001**, *40*, 2582–2586.
- (17) Type D [M_9O_{10}]: (a) Abrahams, I.; Lazell, M.; Motevalli, M.; Shah, S. A. A.; Sullivan, A. C. *J. Organomet. Chem.* **1998**, *553*, 23–29. (b) Ichida, H.; Nagai, K.; Sasaki, Y.; Pope, M. T. *J. Am. Chem. Soc.* **1989**, *111*, 586–591.
- (18) Type D [$M_{10}O_{13}$]: (a) Hayashi, Y.; Ozawa, Y.; Isobe, K. *Inorg. Chem.* **1991**, *30*, 1025–1033. (b) Hayashi, Y.; Ozawa, Y.; Isobe, K. *Chem. Lett.* **1989**, 425–428. (c) Chae, H. K.; Klempner, W. G.; Day, V. W. *Inorg. Chem.* **1989**, *28*, 1423–1424.
- (19) Type E [M_6S_6]: (a) Englich, U.; Chadwick, S.; Ruhlandt-Senge, K. *Inorg. Chem.* **1998**, *37*, 283–293. (b) Chadwick, S.; Englich, U.; Ruhlandt-Senge, K. *Organometallics* **1997**, *16*, 5792–5803. (c) Ruhlandt-Senge, K.; Englich, U. *Chem. Commun.* **1996**, 147–148. (d) Al-Ahmad, S. A.; Salifoglou, A.; Kanatzidis, M. G.; Dunham, W. R.; Coucouvanis, D. *Inorg. Chem.* **1990**, *29*, 927–938. (e) Coucouvanis, D.; Salifoglou, A.; Kanatzidis, M. G.; Dunham, W. R.; Simopoulos, A.; Kostikas, A. *Inorg. Chem.* **1988**, *27*, 4066–4077. (f) Coucouvanis, D.; Kanatzidis, M. G. *J. Am. Chem. Soc.* **1985**, *107*, 5005–5006. (g) Freedman, D.; Melman, J. H.; Emge, T. J.; Brennan, J. G. *Inorg. Chem.* **1998**, *37*, 4162–4163.
- (20) Type E [$M_{13}O_{14}$]: Kondo, M.; Shinagawa, R.; Miyazawa, M.; Kabir, M. K.; Irie, Y.; Horiba, T.; Naito, T.; Maeda, K.; Utsuno, S.; Uchida, F. *Dalton Trans.* **2003**, 515–516.

- (21) Type F [M_8S_8]: (a) Koutmos, M.; Coucouvanis, D. *Inorg. Chem.* **2004**, *43*, 6508–6510. (b) Han, J.; Koutmos, M.; Al Ahmad, S.; Coucouvanis, D. *Inorg. Chem.* **2001**, *40*, 5985–5999. (c) Zhang, Y.; Holm, R. H. *Inorg. Chem.* **2004**, *43*, 674–682. (d) Murata, T.; Gao, H.; Mizobe, Y.; Nakano, F.; Motomura, S.; Tanase, T.; Yano, S.; Hidai, M. *J. Am. Chem. Soc.* **1992**, *114*, 8287–8288.
- (22) Type G [M_8S_8]: (a) Herbst, K.; Monari, M.; Brorson, M. *Inorg. Chem.* **2002**, *41*, 1336–1338. (b) Herbst, K.; Monari, M.; Brorson, M. *Inorg. Chem.* **2001**, *40*, 2979–2985. (c) Christou, G.; Garner, C. D. *J. Chem. Soc., Dalton Trans.* **1980**, 2354–2362. (d) Wolff, T. E.; Power, P. P.; Frankel, R. B.; Holm, R. H. *J. Am. Chem. Soc.* **1980**, *102*, 4694–4703. (e) Wolff, T. E.; Berg, J. M.; Hodgson, K. O.; Frankel, R. B.; Holm, R. H. *J. Am. Chem. Soc.* **1979**, *101*, 4140–4150. (f) Wolff, T. E.; Berg, J. M.; Warrick, C.; Hodgson, K. O.; Holm, R. H. *J. Am. Chem. Soc.* **1978**, *100*, 4630–4632.
- (23) Type H [M_3S_4]: (a) Ide, Y.; Sasaki, M.; Maeyama, M.; Shibahara, T. *Inorg. Chem.* **2004**, *43*, 602–612. (b) Shibahara, T.; Yamasaki, M.; Watase, T.; Ichimura, A. *Inorg. Chem.* **1994**, *33*, 292–301. (c) Akashi, H.; Shibahara, T.; Kuroya, H. *Polyhedron* **1990**, *9*, 1671–1676. (d) Takagi, F.; Seino, H.; Mizobe, Y.; Hidai, M. *Organometallics* **2002**, *21*, 694–699. (e) Müller, A.; Schimanski, U.; Schimanski, J. *Inorg. Chim. Acta* **1983**, *76*, L245–L246. (f) Müller, A.; Reinsch, U. *Angew. Chem., Int. Ed. Engl.* **1980**, *19*, 72–73.
- (24) Type H [M_3O_4]: Müller, A.; Ruck, A.; Dartmann, M.; Reinsch-Vogell, U. *Angew. Chem., Int. Ed. Engl.* **1981**, *20*, 483–484.

Chart 2



There is only one example of the synthesis of a closed capsule-type linked incomplete double cubane sulfide cluster without i with one vacant coordination site (**L** in Chart 2),³² which is regarded as a structural model for the catalytically active site (FeMoco) of Mo-nitrogenase.³³ The half-capsule of **L** can be slid to one side with the change of linkage ligands to give an open capsule-type linked incomplete double cubane sulfide cluster without i , which has two uncovered vacant coordination sites (**M** in Chart 2). However, the synthesis of such an attractive open capsule-type sulfide cluster **M** has yet to be achieved because there has been no systematic strategy for the synthesis of such open capsule-type sulfide clusters without an intramolecular inversion center.

We report herein the first example of a rational synthesis of an open capsule-type octanuclear heterometallic sulfide cluster (M_8S_6 , where M = metal ions) with a linked incomplete double

cubane framework without an intramolecular inversion center as shown as type **M** in Chart 2: $[Ru(\eta^6-C_6Me_6)\{P(OMe)_3\}-\{MoO(\mu_3-S)_3\}(CuI)_2]_2$ (**5**). Scheme 1 summarizes our strategy to synthesize the open capsule-type M_8S_6 cluster **5** by stepwise connection of three mononuclear building blocks: $[RuCl_2(\eta^6-C_6Me_6)\{P(OMe)_3\}]$ (**1a**, mononuclear) $\rightarrow [Ru(\eta^6-C_6Me_6)\{P(OMe)_3\}\{MoOS(\mu_2-S)_2\}]$ (**2a**, dinuclear) $\rightarrow [Ru(\eta^6-C_6Me_6)\{P(OMe)_3\}\{MoO(\mu_2-S)_2(\mu_3-S)\}CuI]$ (**3a**, butterfly-type trinuclear) \rightarrow a mixture of two incomplete double cubane-type octanuclear sulfide clusters with or without an intramolecular inversion center $[Ru(\eta^6-C_6Me_6)\{P(OMe)_3\}\{MoO(\mu_3-S)_3\}(CuI)_2]_2$ (**4** or **5**, respectively), which were separated by recrystallization. When $P(OMe)_3$ was replaced by $P(OEt)_3$ in the starting ruthenium building block $[RuCl_2(\eta^6-C_6Me_6)\{P(OEt)_3\}]$ (**1b**, mononuclear), only the tetranuclear incomplete single cubane cluster $[Ru(\eta^6-C_6Me_6)\{P(OEt)_3\}\{MoO(\mu_3-S)_3\}(CuI)_2]$ (**6**) was formed due to the steric effect of $P(OEt)_3$, which is more bulky than $P(OMe)_3$ (Scheme 1). The structures of **1a**, **2a**, **3a**, **3b**, **4**, **5**, and **6** were determined by X-ray analysis.

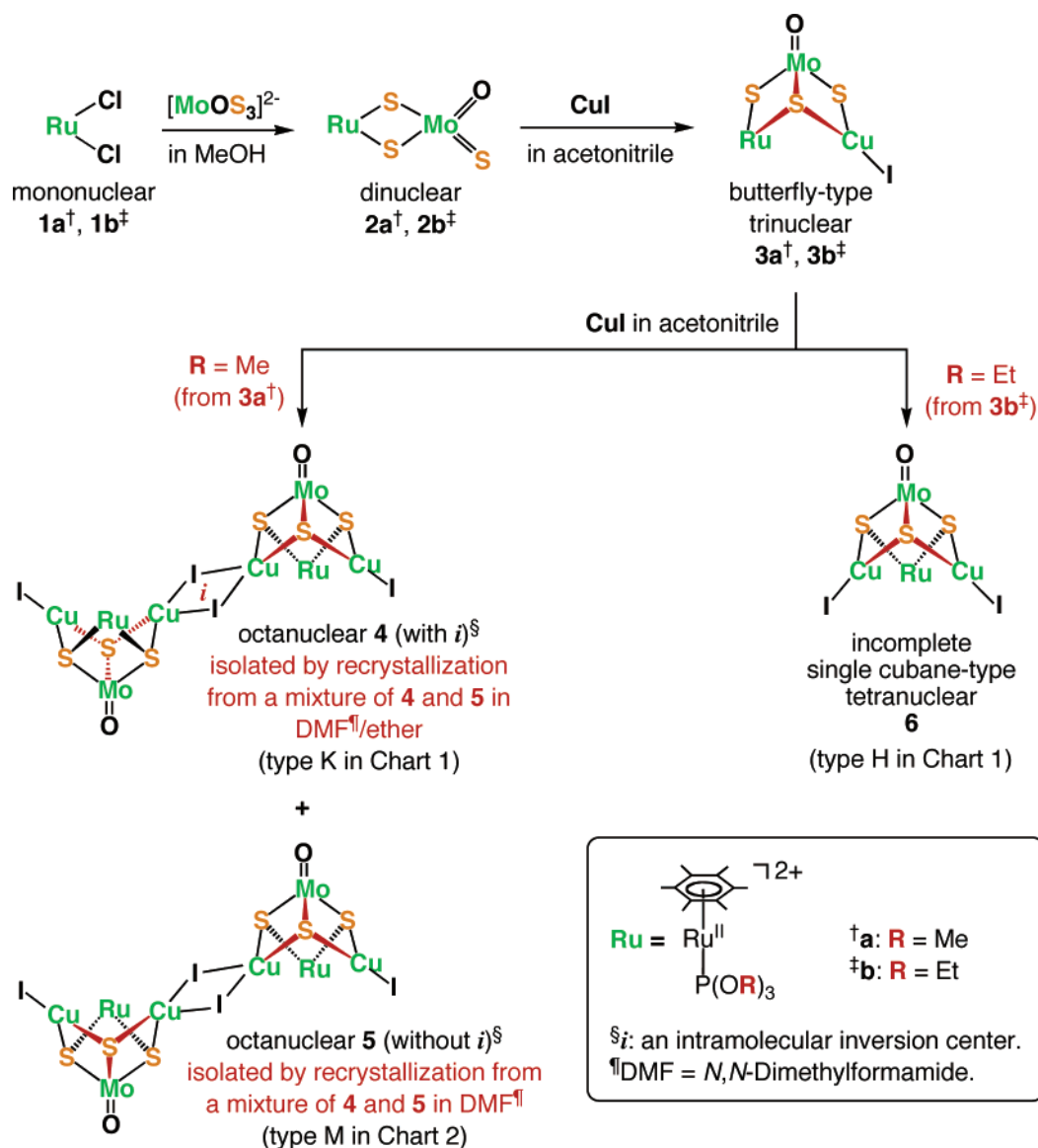
Experimental Section

Materials and Methods. Compounds **1a**, **1b**, **2a**, **2b**, **3a**, **3b**, **4**, **5**, and **6** are stable to air. All preparative procedures were routinely carried out under an atmospheric pressure of Ar. Methanol, hexane, acetonitrile, *N,N*-dimethylformamide (DMF), diethyl ether, dichloromethane, and chloroform were purchased from Wako Pure Chemical Industries, Ltd. and were used without further purification. Trimethyl phosphite, triethyl phosphite, and CuI were purchased from Wako Pure Chemical Industries and were used without further purification. $[RuCl_2(\eta^6-C_6Me_6)\{P(OMe)_3\}]$ (**1a**) and $[NH_4]_2[MoOS_3]$ were prepared by the methods described in the literature.^{34,35} $[Ph_4P]_2[MoOS_3]$ was synthesized from $[NH_4]_2[MoOS_3]$ by a method similar to that for $[Ph_4P]_2[MoS_4]$ and by the method described in the literature.³⁶ 1H NMR spectra were recorded on a JEOL 300 MHz spectrometer (JNM-AL 300) and reported in ppm vs tetramethylsilane (TMS). IR spectra of solid compounds as KBr disks were recorded on a Thermo Nicolet NEXUS 870 FT-IR instrument using 2 cm^{-1} standard resolution at ambient temperature. ESI-MS data were collected on an API 365 triple quadrupole mass spectrometer (PE-Sciex) in positive detection mode, equipped with an

- (25) Type **H** $[M_4S_3]$: (a) Coucouvanis, D.; Han, J.; Moon, N. *J. Am. Chem. Soc.* **2002**, *124*, 216–224. (b) Han, J.; Beck, K.; Ockwig, N.; Coucouvanis, D. *J. Am. Chem. Soc.* **1999**, *121*, 10448–10449. (c) Tyson, M. A.; Coucouvanis, D. *Inorg. Chem.* **1997**, *36*, 3808–3809. (d) Chu, C. T.-W.; Dahl, L. F. *Inorg. Chem.* **1977**, *16*, 3245–3251. (e) Atencio, R.; Casado, M. A.; Ciriano, M. A.; Lahoz, F. J.; Pérez-Torrente, J. J.; Tiripicchio, A.; Oro, L. A. *J. Organomet. Chem.* **1996**, *514*, 103–110.
- (26) Type **I** $[M_4O_6]$: (a) Takara, S.; Ogo, S.; Watanabe, Y.; Nishikawa, K.; Kinoshita, I.; Isobe, K. *Angew. Chem., Int. Ed.* **1999**, *38*, 3051–3053. $[M_5O_6]$: (b) Do, Y.; You, X.-Z.; Zhang, C.; Ozawa, Y.; Isobe, K. *J. Am. Chem. Soc.* **1991**, *113*, 5892–5893.
- (27) Type **I** $[M_7O_{12}]$: Khan, M. I.; Tabussum, S.; Doedens, R. *J. Chem. Commun.* **2003**, 532–533.
- (28) Type **I** $[M_8O_{10}]$: Nishikawa, K.; Kido, K.; Yoshida, J.; Nishioka, T.; Kinoshita, I.; Breedlove, B. K.; Hayashi, Y.; Uehara, A.; Isobe, K. *Appl. Organomet. Chem.* **2003**, *17*, 446–448.
- (29) Type **J** $[M_6S_5]$: (a) Snyder, B. S.; Reynolds, M. S.; Holm, R. H. *Polyhedron* **1991**, *10*, 203–213. (b) Snyder, B. S.; Holm, R. H. *Inorg. Chem.* **1990**, *29*, 274–279. (c) Snyder, B. S.; Holm, R. H. *Inorg. Chem.* **1988**, *27*, 2339–2347. (d) Reynolds, M. S.; Holm, R. H. *Inorg. Chem.* **1988**, *27*, 4494–4499. (e) Chen, C.; Cai, J.; Liu, Q.; Wu, D.; Lei, X.; Zhao, K.; Kang, B.; Lu, J. *Inorg. Chem.* **1990**, *29*, 4878–4881.
- (30) Type **J** $[M_6S_4O]$: Casado, M. A.; Ciriano, M. A.; Edwards, A. J.; Lahoz, F. J.; Pérez-Torrente, J. J.; Oro, L. A. *Organometallics* **1998**, *17*, 3414–3416.
- (31) Type **K** $[M_8S_6]$: (a) Osterloh, F.; Achim, C.; Holm, R. H. *Inorg. Chem.* **2001**, *40*, 224–232. (b) Lang, J.; Kawaguchi, H.; Ohnishi, S.; Tatsumi, K. *Chem. Commun.* **1997**, 405–406. (c) Lang, J.-P.; Xu, Q.-F.; Chen, Z.-N.; Abrahams, B. F. *J. Am. Chem. Soc.* **2003**, *125*, 12682–12683. (d) Beheshti, A.; Clegg, W.; Hyvadi, R.; Hekmat, H. F. *Polyhedron* **2002**, *21*, 1547–1552. (e) Ogo, S.; Suzuki, T.; Ozawa, Y.; Isobe, K. *Inorg. Chem.* **1996**, *35*, 6093–6101.
- (32) Type **L** $[M_8S_6]$: Li, Z.; Du, S.; Wu, X. *Dalton Trans.* **2004**, 2438–2443.
- (33) Spectroscopic and theoretical studies have shown that the $M-X$ (M = metal ions) bonds are disrupted during catalysis to form a closed capsule-type heterometallic sulfide cluster with linked incomplete double cubane (M_8S_6) frameworks without an intramolecular inversion center. (a) Vela, J.; Stoian, S.; Flaschenriem, C. J.; Münck, E.; Holland, P. L. *J. Am. Chem. Soc.* **2004**, *126*, 4522–4523. (b) Schimpl, J.; Petrilli, H. M.; Blöchl, P. E. *J. Am. Chem. Soc.* **2003**, *125*, 15772–15778.

- (34) (a) Werner, H.; Kletzin, H.; Roder, K. *J. Organomet. Chem.* **1988**, *355*, 401–417. (b) Klauui, W.; Buchholz, E. *Inorg. Chem.* **1988**, *27*, 3500–3506.
- (35) (a) McDonald, J. W.; Friesen, G. D.; Rosenhein, L. D.; Newton, W. E. *Inorg. Chim. Acta* **1983**, *72*, 205–210. (b) Harmer, M. A.; Sykes, G. *Inorg. Chem.* **1980**, *19*, 2881–2885.
- (36) Hadjikyriacou, A. I.; Coucouvanis, D. *Inorg. Synth.* **1990**, *27*, 39.

Scheme 1



ion spray interface. The sprayer was held at a potential of +5.0 kV, and compressed N_2 was employed to assist liquid nebulization.

[RuCl $_2$ (η^6 -C $_6$ Me $_6$){P(OEt) $_3$ }] (1b). A suspension of [RuCl(η^6 -C $_6$ -Me $_6$)(μ -Cl) $_2$ (1.00 g, 2.00 mmol) and triethyl phosphite (5 cm 3) in dichloromethane (150 cm 3) was refluxed for 1 h. A dark red solution was filtered and evaporated to dryness. Recrystallization of the solid residue from dichloromethane/hexane gave dark red crystals. A product was collected by filtration and dried in vacuo. Yield: 96% based on [RuCl(η^6 -C $_6$ Me $_6$)(μ -Cl) $_2$]. Anal. Calcd for C $_{18}$ H $_{33}$ Cl $_2$ O $_3$ PRu: C, 43.20; H, 6.65%. Found: C, 43.19; H, 6.37. 1H NMR (CDCl $_3$, 23 $^\circ C$): δ 1.26 (t, $^3J_{H,H} = 6.9$ Hz, 9H, $-CH_2CH_3$), 2.03 (d, $^4J_{P,H} = 1.2$ Hz, 18H, $-CH_3(\eta^6$ -C $_6$ Me $_6$)), 4.14 (dq, $^3J_{P,H} = 6.9$ Hz, $^3J_{H,H} = 6.9$ Hz, 6H, $-CH_2-$).

[Ru(η^6 -C $_6$ Me $_6$){P(OMe) $_3$ }{MoOS(μ_2 -S) $_2$ }] (2a). A methanol solution (50 cm 3) of **1a** (0.69 g, 1.51 mmol) was added to a methanol solution (250 cm 3) of [Ph $_4$ P] $_2$ [MoOS $_3$] (1.37 g, 1.54 mmol) at room temperature. The mixture was stirred for 12 h to yield purple crystals of **2a**, which were collected by filtration, washed with methanol (3 \times 30 cm 3) and diethyl ether (3 \times 20 cm 3), and dried in vacuo. Crystals of **2a** were further obtained by evaporating the filtrate to ca. 100 cm 3 below 30 $^\circ C$. Yield: 87% based on **1a**. Anal. Calcd for C $_{15}$ H $_{27}$ MoO $_4$ -PRuS $_3$: C, 30.25; H, 4.57%. Found: C, 29.96; H, 4.31%. 1H NMR

(CDCl $_3$, 23 $^\circ C$): δ 1.97 (d, $^4J_{P,H} = 1.2$ Hz, 18H, $-CH_3(\eta^6$ -C $_6$ Me $_6$)), 3.68 (d, $^3J_{P,H} = 10.5$ Hz, 9H, $-OCH_3$).

[Ru(η^6 -C $_6$ Me $_6$){P(OEt) $_3$ }{MoO(μ_2 -S) $_2$ }] (2b). Complex **2b** was similarly prepared from **1b** in 89% yield based on **1b**. Anal. Calcd for C $_{18}$ H $_{33}$ MoO $_4$ PRuS $_3$: C, 33.90; H, 5.22%. Found: C, 33.61; H, 4.92%. 1H NMR (CDCl $_3$, 23 $^\circ C$): δ 1.20 (t, $^3J_{H,H} = 6.9$ Hz, 9H, $-CH_2CH_3$), 1.23 (t, $^3J_{H,H} = 6.9$ Hz, 9H, $-CH_2CH_3$), 2.21 (d, $^4J_{P,H} = 0.9$ Hz, 18H, $-CH_3(\eta^6$ -C $_6$ Me $_6$)), 2.28 (d, $^4J_{P,H} = 0.9$ Hz, 18H, $-CH_3(\eta^6$ -C $_6$ Me $_6$)), 3.88 (dq, $^3J_{P,H} = 6.9$ Hz, $^3J_{H,H} = 6.9$ Hz, 6H, $-CH_2-$), 3.99 (dq, $^3J_{P,H} = 6.9$ Hz, $^3J_{H,H} = 6.9$ Hz, 6H, $-CH_2-$).

[Ru(η^6 -C $_6$ Me $_6$){P(OMe) $_3$ }{MoO(μ_2 -S) $_2$ (μ_3 -S)}CuI] (3a). Cluster **3a** was obtained from a reaction of **2a** (0.32 g, 0.54 mmol) with CuI (0.10 g, 0.54 mmol) in acetonitrile (60 cm 3). After stirring for 12 h at room temperature, the mixture was concentrated to ca. 20 cm 3 giving a purple precipitate, which was collected by filtration, washed with a small amount of diethyl ether, and dried in vacuo (Yield: 93% based on **2a**). Anal. Calcd for C $_{15}$ H $_{27}$ CuIMoO $_4$ PRuS $_3$: C, 22.92; H, 3.46%. Found: C, 23.00; H, 3.29%. 1H NMR (CD $_3$ CN, 23 $^\circ C$): δ 2.26 (d, $^4J_{P,H} = 1.2$ Hz, 18H, $-CH_3(\eta^6$ -C $_6$ Me $_6$)), 3.23 (d, $^3J_{P,H} = 11.1$ Hz, 9H, $-OCH_3$).

[Ru(η^6 -C $_6$ Me $_6$){P(OEt) $_3$ }{MoO(μ_2 -S) $_2$ (μ_3 -S)}CuI] (3b). Complex **3b** was similarly prepared from **2b** in 87% yield based on **2b**. Anal.

Calcd for $C_{18}H_{33}MoO_4PRuS_3$: C, 26.11; H, 4.02%. Found: C, 25.93; H, 4.25%. 1H NMR (CD_3CN , 23 °C): δ 1.16 (t, $^3J_{HH} = 6.9$ Hz, 9H, $-CH_2CH_3$), 2.24 (d, $^4J_{P,H} = 1.2$ Hz, 18H, $-CH_3(\eta^6-C_6Me_6)$), 3.78 (dq, $^3J_{P,H} = 6.9$ Hz, $^3J_{H,H} = 6.9$ Hz, 6H, $-CH_2-$).

[Ru($\eta^6-C_6Me_6$){P(OMe) $_3$ }{MoO(μ_3-S) $_3$ }(CuI) $_2$] (4, with an Inversion Center). Method A. CuI (0.053 g, 0.30 mmol) was added to an acetonitrile solution (100 cm^3) of **3a** (0.20 g, 0.25 mmol) at room temperature. After stirring for 12 h at room temperature, the mixture was concentrated to ca. 50 cm^3 giving a purple precipitate, which was collected by filtration, washed with a small amount of diethyl ether, and dried in vacuo. Dark red block crystals of **4** were obtained from a DMF/diethyl ether solution of the purple precipitate. Yield: 40% based on **3a**. Anal. Calcd for $C_{30}H_{54}Cu_4I_4Mo_2O_8P_2Ru_2S_6$: C, 18.45; H, 2.79%. Found: C, 18.71; H, 2.61%. 1H NMR (CD_3CN , 23 °C): δ 2.31 (d, $^4J_{P,H} = 1.2$ Hz, 18H, $-CH_3(\eta^6-C_6Me_6)$), 3.43 (d, $^3J_{P,H} = 11.7$ Hz $-OCH_3$). **Method B.** Cluster **4** was obtained from a reaction of **2a** (0.30 g, 0.50 mmol) with CuI (0.20 g, 1.05 mmol) in acetonitrile (100 cm^3). After stirring for 12 h at room temperature, the mixture was concentrated to 50 cm^3 to give a purple precipitate, which was collected by filtration, washed with a small amount of diethyl ether, and dried in vacuo. Dark red block crystals of **4** were obtained from a DMF/diethyl ether solution of the purple precipitate. Yield: 44% based on **2a**.

[Ru($\eta^6-C_6Me_6$){P(OMe) $_3$ }{MoO(μ_3-S) $_3$ }(CuI) $_2$] (5, without an Inversion Center). Cluster **5** was prepared in the same manner as **4**. Dark red platelet crystals of **5** were obtained from a DMF solution of the purple precipitate. Yield: 40% based on **3a**. Anal. Calcd for $C_{30}H_{54}Cu_4I_4Mo_2O_8P_2Ru_2S_6$: C, 18.45; H, 2.79%. Found: C, 18.71; H, 2.61%. 1H NMR (CD_3CN , 23 °C): δ 2.31 (d, $^4J_{P,H} = 1.2$ Hz, 18H, $-CH_3(\eta^6-C_6Me_6)$), 3.43 (d, $^3J_{P,H} = 11.7$ Hz $-OCH_3$).

[Ru($\eta^6-C_6Me_6$){P(OEt) $_3$ }{MoO(μ_3-S) $_3$ }(CuI) $_2$] (6). Cluster **6** was obtained from a reaction of **3b** (0.20 g, 0.25 mmol) with CuI (0.053 g, 0.30 mmol) in acetonitrile (100 cm^3). After stirring for 12 h at room temperature, the mixture was concentrated to ca. 50 cm^3 giving a purple precipitate, which was collected by filtration, washed with a small amount of diethyl ether, and dried in vacuo (Yield: 94% based on **3b**). Anal. Calcd for $C_{18}H_{33}I_2Cu_2MoO_4PRuS_3$: C, 21.22; H, 3.27%. Found: C, 20.95; H, 3.05%. 1H NMR (CD_3CN , 23 °C): δ 1.19 (t, $^3J_{HH} = 6.9$ Hz, 9H, $-CH_2CH_3$), 2.29 (d, $^4J_{P,H} = 1.2$ Hz, 18H, $-CH_3(\eta^6-C_6Me_6)$), 3.75 (dq, $^3J_{P,H} = 6.9$ Hz, $^3J_{H,H} = 6.9$ Hz, 6H, $-CH_2-$).

X-ray Crystallographic Analysis. Crystallographic data for **1a**,³⁷ **2a**,³⁸ **3a**,³⁹ **3b**,⁴⁰ **4**,⁴¹ **5**,⁴² and **6**⁴³ have been deposited with the Cambridge Crystallographic Data Center as supplementary publication No. CCDC-266125, 266126, 240914, 266127, 266128, 240913, and 266129,

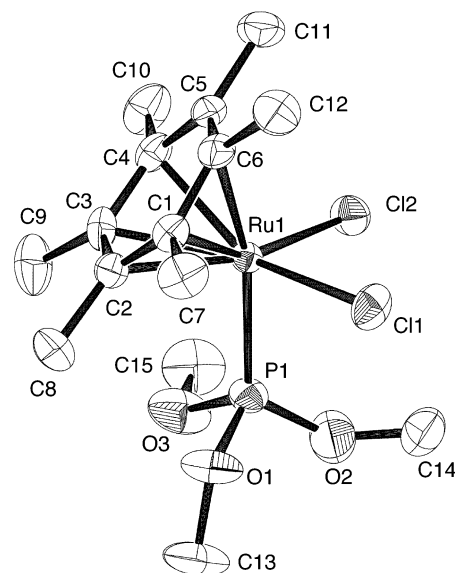


Figure 1. ORTEP drawing of **1a**. Selected bond lengths (\AA) and angles (ϕ/deg): Ru1–C1 = 2.207(3), Ru1–C2 = 2.227(3), Ru1–C3 = 2.248(3), Ru1–C4 = 2.216(3), Ru1–C5 = 2.288(3), Ru1–C6 = 2.284(3), C1–C6 = 1.433(5), C4–C5 = 1.437(5), C5–C6 = 1.402(5), Ru1–Cl1 = 2.4138(9), Ru1–Cl2 = 2.4042(9), Ru1–P1 = 2.2678(9), P1–Ru1–Cl1 = 86.51(3), P1–Ru1–Cl2 = 86.17(4), Cl1–Ru1–Cl2 = 88.84(3).

respectively. Copies of the data can be obtained free of charge on application to CCDC, 12 Union Road, Cambridge CB21EZ, UK {Fax: (+44)1223-336-033. E-mail: deposit@ccdc.cam.ac.uk}. Measurements were made on a Rigaku/MSC Mercury CCD diffractometer with graphite monochromated Mo $K\alpha$ radiation ($\lambda = 0.7107$ \AA). Data were collected and processed using the CrystalClear program (Rigaku). All calculations were performed using the teXsan crystallographic software package of Molecular Structure Corporation. An ORTEP drawing of **3b** is shown in Figure S1 (in the Supporting Information).

Results and Discussion

Synthesis and Structures of [RuCl $_2$ ($\eta^6-C_6Me_6$){P(OR) $_3$]} {R = Me (1a), Et (1b)}. Complexes **1a** and **1b** were prepared from the reaction of $[RuCl_2(\eta^6-C_6Me_6)(\mu-Cl)]_2$ with P(OR) $_3$ {R = Me(**1a**), Et(**1b**)} in dichloromethane.³⁴ Red crystals of **1a** used in X-ray analysis (Figure 1) were obtained from mixed solvents of dichloromethane/diethyl ether. The Ru atom has an octahedral coordination geometry with bonding parameters similar to $[RuCl_2(\eta^6-C_6Me_6)(PMe_3)]$.⁴⁴ The distances between Ru atom and carbons of the $\eta^6-C_6Me_6$ ring of complex **1a** in the solid state are not equivalent: the distances of Ru–C5 and Ru–C6 {2.288(3) and 2.284(3) \AA , respectively} trans to the P(OMe) $_3$ ligand are longer than those of Ru–C1, Ru–C2, Ru–C3, and Ru–C4 {2.207(3), 2.227(3), 2.248(3), and 2.216(3) \AA , respectively} trans to the Cl ligands. This indicates that the P(OMe) $_3$ ligand has a greater trans influence than the Cl ligands. Thus, the bond distance of C5–C6 {1.402(5) \AA } of the $\eta^6-C_6Me_6$ ring is shorter than those of C1–C6 and C4–C5 {1.433(5) and 1.437(5) \AA , respectively}.

Synthesis and Structures of [Ru($\eta^6-C_6Me_6$){P(OR) $_3$ }{MoOS(μ_2-S) $_2$]} {R = Me (2a), Et (2b)}. The molecular structure of the dinuclear sulfide complex **2a** determined by X-ray analysis is shown in Figure 2. Red crystals of **2a** used in the X-ray analysis were obtained from mixed solvents of chloroform/diethyl ether. Ru and Mo atoms have octahedral and

(44) Hansen, H. D.; Nelson, J. H. *Organometallics* **2000**, *19*, 4740–4755.

- (37) Crystal data for **1a**·0.5CH $_2$ Cl $_2$: $C_{15.50}H_{28}Cl_3O_3PRu$, MW 500.79, monoclinic, space group $C2/c$ (No. 15), $a = 15.536(2)$ \AA , $b = 9.1070(8)$ \AA , $c = 28.617(3)$ \AA , $\beta = 95.150(4)^\circ$, $V = 4032.4(7)$ \AA^3 , $Z = 8$, $D_C = 1.650$ $g\ cm^{-3}$, $\mu(\text{Mo } K\alpha) = 12.65$ cm^{-1} , $T = 173$ K, $R1 = 0.036$, and $R_w = 0.095$.
- (38) Crystal data for **2a**: $C_{15}H_{27}MoO_4PRuS_3$, MW 595.54, orthorhombic, space group $Cmc2_1$ (No. 36), $a = 9.449(6)$ \AA , $b = 16.93(1)$ \AA , $c = 13.252(8)$ \AA , $V = 2119(2)$ \AA^3 , $Z = 4$, $D_C = 1.866$ $g\ cm^{-3}$, $\mu(\text{Mo } K\alpha) = 16.91$ cm^{-1} , $T = 223$ K, $R1 = 0.040$, and $R_w = 0.088$.
- (39) Crystal data for **3a**·0.7CH $_3$ CN: $C_{16.40}H_{29.10}CuI_2MoO_4PRuS_3$, MW 814.73, monoclinic, space group $P2_1/n$ (No. 14), $a = 8.934(4)$ \AA , $b = 23.350(9)$ \AA , $c = 13.258(7)$ \AA , $\beta = 96.171(7)^\circ$, $V = 2749(2)$ \AA^3 , $Z = 4$, $D_C = 1.968$ $g\ cm^{-3}$, $\mu(\text{Mo } K\alpha) = 31.87$ cm^{-1} , $T = 173$ K, $R1 = 0.058$, and $R_w = 0.160$.
- (40) Crystal data for **3b**: $C_{18}H_{33}CuI_2MoO_4PRuS_3$, MW 828.07, monoclinic, space group $P2_1/n$ (No. 14), $a = 16.036(9)$ \AA , $b = 11.237(6)$ \AA , $c = 15.621(9)$ \AA , $\beta = 93.755(9)^\circ$, $V = 2808(2)$ \AA^3 , $Z = 4$, $D_C = 1.958$ $g\ cm^{-3}$, $\mu(\text{Mo } K\alpha) = 31.21$ cm^{-1} , $T = 223$ K, $R1 = 0.057$, and $R_w = 0.145$.
- (41) Crystal data for **4**·DMF: $C_{18}H_{34}Cu_2I_2MoNO_3PRuS_3$, MW 1049.54, monoclinic, space group $C2/c$ (No. 15), $a = 37.63(2)$ \AA , $b = 9.293(4)$ \AA , $c = 19.393(9)$ \AA , $\beta = 110.535(5)^\circ$, $V = 6350(4)$ \AA^3 , $Z = 8$, $D_C = 2.195$ $g\ cm^{-3}$, $\mu(\text{Mo } K\alpha) = 43.94$ cm^{-1} , $T = 173$ K, $R1 = 0.053$, and $R_w = 0.165$.
- (42) Crystal data for **5**: $C_{15}H_{27}Cu_2I_2MoO_4PRuS_3$, MW 976.44, monoclinic, space group $C2/c$ (No. 15), $a = 9.545(2)$ \AA , $b = 18.288(3)$ \AA , $c = 31.466(6)$ \AA , $\beta = 97.5020(7)^\circ$, $V = 5445.0(9)$ \AA^3 , $Z = 8$, $D_C = 2.382$ $g\ cm^{-3}$, $\mu(\text{Mo } K\alpha) = 51.11$ cm^{-1} , $T = 173$ K, $R1 = 0.042$, and $R_w = 0.085$.
- (43) Crystal data for **6**: $C_{18}H_{33}Cu_2I_2MoO_4PRuS_3$, MW 1018.52, monoclinic, space group $P2_1/n$ (No. 14), $a = 9.395(4)$ \AA , $b = 16.327(7)$ \AA , $c = 19.521(9)$ \AA , $\beta = 95.777(5)^\circ$, $V = 2979(2)$ \AA^3 , $Z = 4$, $D_C = 2.271$ $g\ cm^{-3}$, $\mu(\text{Mo } K\alpha) = 46.76$ cm^{-1} , $T = 223$ K, $R1 = 0.046$, and $R_w = 0.119$.

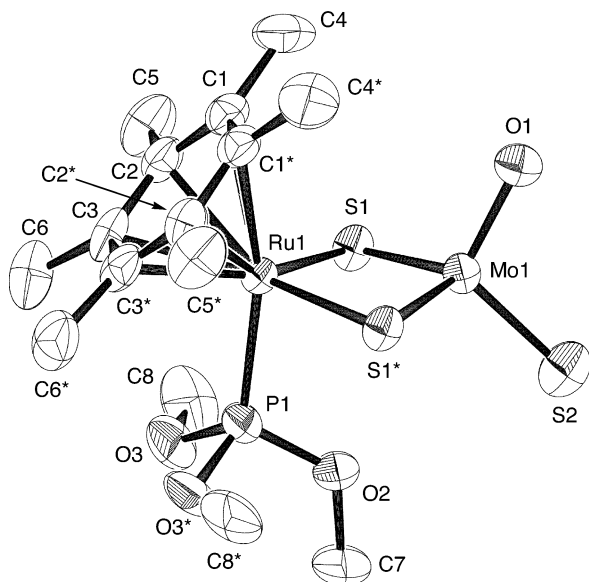


Figure 2. ORTEP drawing of **2a**. Selected interatomic distances (\AA) and angles ($^\circ$): Ru1–Mo1 = 2.924(1), Ru1–S1 = 2.388(2), Mo1–S1 = 2.247(2), Mo1–S2 = 2.121(5), Mo1–O1 = 1.80(1), Ru1–S1–Mo1 = 78.16(8), Ru1–Mo1–S2 = 136.1(2), Ru1–Mo1–O1 = 115.4(3), S1–Mo1–O1 = 110.0(2), S2–Mo1–O1 = 108.6(4).

tetrahedral coordination geometries, respectively. The Ru \cdots Mo distance, 2.924(1) \AA , is similar to that of the trinuclear sulfide cluster $[\text{Ru}\{\text{CO}(\text{PhNCHS})(\text{PPh}_3)(\mu\text{-S})_2\}_2\text{Mo}] \{2.8646(8) \text{\AA}\}$.⁴⁵ The Mo–S (bridge) bond distances (av. 2.247 \AA) are considerably longer than the Mo–S3 (terminal) bond distance in **2a** {2.121(5) \AA } and in $\text{Cs}_2[\text{MoOS}_3]$ (2.178 \AA) with some double bond character.^{46a} The Mo–O bond distance {1.80(1) \AA } is in the normal double bond distances range. An infrared spectrum of complex **2a**, therefore, exhibits two $\nu_{\text{Mo-S}}$ bands, one for Mo–S (bridge) (450 cm^{-1}) and the other for Mo–S (terminal) (494 cm^{-1}), and one $\nu_{\text{Mo-O}}$ band (899 cm^{-1}).⁴⁶ The Ru–Mo–O1 angle {115.4(3) $^\circ$ } of **2a** is smaller than Ru–Mo–S2 {136.1(2) $^\circ$ } owing to the steric effect of the trimethyl phosphite group. An infrared spectrum of complex **2b** also exhibits two $\nu_{\text{Mo-S}}$ bands, one for Mo–S (bridge) (457 cm^{-1}) and the other for Mo–S (terminal) (497 cm^{-1}), and one $\nu_{\text{Mo-O}}$ band (897 cm^{-1}).

Synthesis and Structures of $[\text{Ru}(\eta^6\text{-C}_6\text{Me}_6)\{\text{P}(\text{OR})_3\}\{\text{MoO}(\mu_2\text{-S})_2(\mu_3\text{-S})\}\text{CuI}]\{\text{R} = \text{Me} (\mathbf{3a}), \text{Et} (\mathbf{3b})\}$. An ORTEP drawing of **3a** is shown in Figure 3. Red crystals of **3a** used in the X-ray analysis were obtained from mixed solvents of acetonitrile/diethyl ether. The trinuclear cluster **3a** has a butterfly-type framework, in which the Ru, Mo, and Cu atoms are arranged in a right-angled fashion {Ru1–Mo1–Cu1 = 91.89(5) $^\circ$ }, and the S2 atom has a μ_3 -coordination mode. There are a few reports on such M_3S_3 butterfly-type mixed metal clusters.^{23f,31e} The Ru, Mo, and Cu atoms have octahedral, tetrahedral, and trigonal planar coordination geometries, respectively. The Mo–S2 (μ_3) bond distance {2.277(3) \AA } is longer than the Mo–S1 (μ_2) and Mo–S3 (μ_2) bond distances {2.233(3) \AA and 2.208(4) \AA , respectively}. Thus, the IR

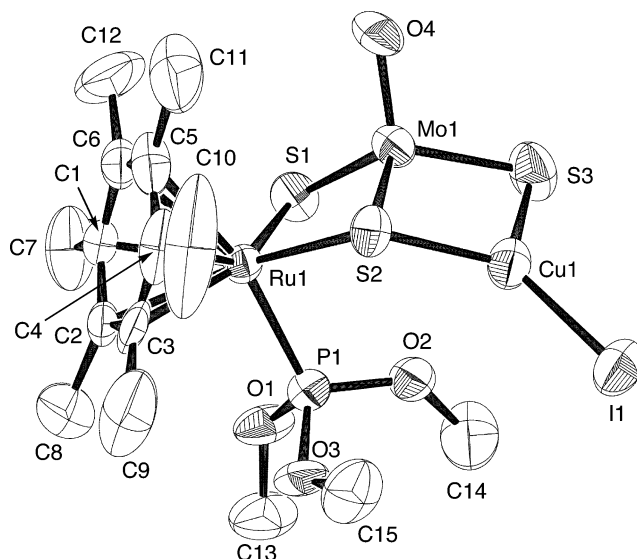


Figure 3. ORTEP drawing of **3a**. Selected interatomic distances (\AA) and angles ($^\circ$): Ru1–Mo1 = 2.885(2), Mo1–Cu1 = 2.655(2), Ru1–S1 = 2.372(3), Ru1–S2 = 2.382(3), Mo1–S1 = 2.233(3), Mo1–S2 = 2.277(3), Mo1–S3 = 2.208(4), Mo1–O4 = 1.714(9), Cu1–I1 = 2.453(2), Ru1–S1–Mo1 = 77.49(9), Ru1–S2–Mo1 = 76.48(9), Ru1–S2–Cu1 = 117.9(1), S1–Mo1–O4 = 111.0(3), S2–Mo1–O4 = 111.9(4), S3–Mo1–O4 = 110.5(3), Mo1–S2–Cu1 = 71.48(9), Mo1–S3–Cu1 = 73.5(1), S2–Cu1–S3 = 107.1(1).

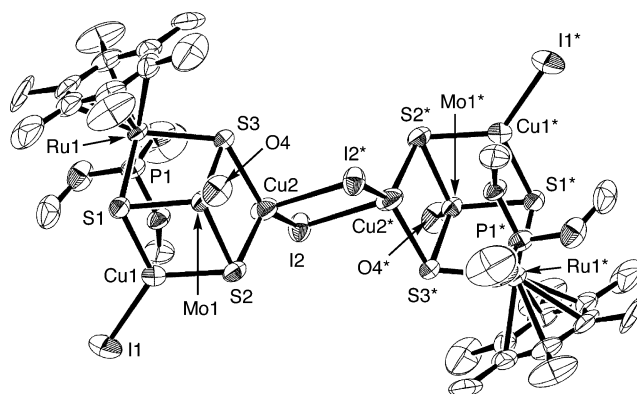


Figure 4. ORTEP drawing of **4**. Selected interatomic distances (\AA) and angles ($^\circ$): Ru1–Mo1 = 2.883(1), Mo1–Cu1 = 2.672(2), Mo1–Cu2 = 2.687(2), Ru1–S1 = 2.376(3), Ru1–S3 = 2.383(2), Mo1–S1 = 2.272(3), Mo1–S2 = 2.283(3), Mo1–S3 = 2.265(3), Mo1–O4 = 1.693(7), Cu1–I1 = 2.459(2), Cu2–I2 = 2.514(2), Cu2–I2* = 2.972(2), Ru1–S1–Mo1 = 76.64(8), Ru1–S3–Mo1 = 76.30(8), Ru1–S1–Cu1 = 117.9(1), Ru1–S3–Cu2 = 124.3(1), S1–Mo1–O4 = 111.3(3), S2–Mo1–O4 = 111.1(3), S3–Mo1–O4 = 113.5(3), Mo1–S1–Cu1 = 72.18(8), Mo1–S3–Cu2 = 71.66(8), S1–Cu1–S2 = 108.0(1), S2–Cu2–S3 = 106.8(1), I2–Cu2–I2* = 100.44(5).

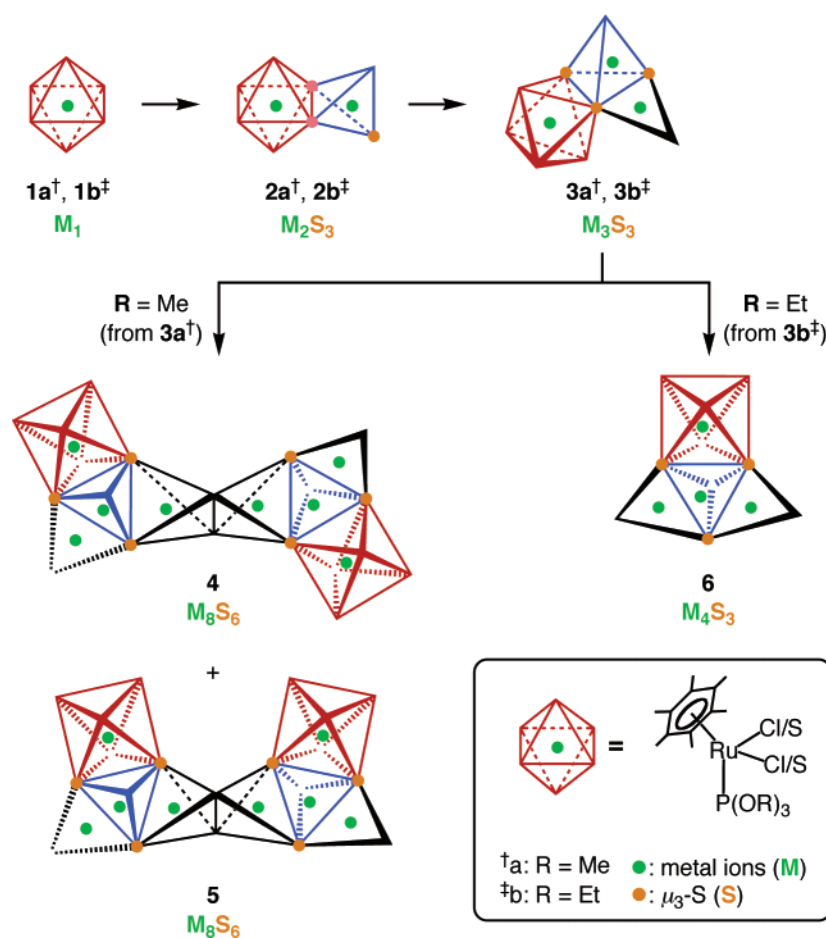
spectrum as a KBr disk of **3a** shows three $\nu_{\text{Mo-S}}$ bands at 467, 471, and 474 cm^{-1} and one $\nu_{\text{Mo-O}}$ band at 914 cm^{-1} . The trinuclear butterfly-type cluster **3b** was also synthesized from a reaction of **2b** with CuI. Red crystals of **3b** used in the X-ray analysis were similarly obtained from a DMF solution of **3b** (Figure S1 in the Supporting Information). The IR spectrum as a KBr disk of **3b** shows three $\nu_{\text{Mo-S}}$ bands at 446, 457, and 465 cm^{-1} and one $\nu_{\text{Mo-O}}$ band at 915 cm^{-1} .

Synthesis and Structure of $[\text{Ru}(\eta^6\text{-C}_6\text{Me}_6)\{\text{P}(\text{OMe})_3\}\{\text{MoO}(\mu_3\text{-S})_3\}(\text{CuI})_2]$ (4** with an Inversion Center).** The butterfly-type trinuclear sulfide cluster **3a** was transformed into a mixture of two incomplete double cubane-type octanuclear sulfide clusters $[\text{Ru}(\eta^6\text{-C}_6\text{Me}_6)\{\text{P}(\text{OMe})_3\}\{\text{MoO}(\mu_3\text{-S})_3\}(\text{CuI})_2]$

(45) Kato, M.; Kawano, M.; Taniguchi, H.; Funaki, M.; Moriyama, H.; Sato, T.; Matsumoto, K. *Inorg. Chem.* **1992**, *31*, 26–35.

(46) (a) Müller, A.; Diemann, E.; Jostes, R.; Bögge, H. *Angew. Chem., Int. Ed. Engl.* **1981**, *20*, 934–955. (b) Schmidt, K. H.; Müller, A. *Coord. Chem. Rev.* **1974**, *14*, 115–179. (c) Diemann, E.; Müller, A. *Coord. Chem. Rev.* **1973**, *10*, 79–122. (d) Zhang, C. Z.; Jin, G.-C.; Chen, J.-X.; Xin, X.-Q.; Qian, K.-P. *Coord. Chem. Rev.* **2001**, *213*, 51–77. (e) Nakamoto, K. *Infrared and Raman Spectra of Inorganic and Coordination Compounds*, 5th ed.; John Wiley & Sons: New York, 1997.

Scheme 2



with an intramolecular inversion center (**4**) and without an intramolecular inversion center (**5**), which were separated by recrystallization as shown in Scheme 1. Red crystals used in the X-ray analysis of **4** were obtained from a DMF/diethyl ether solution of the mixture of **4** and **5**. As depicted in Figure 4, cluster **4** has a linked incomplete double cubane-type octanuclear framework with a crystallographic inversion center (type **K** in Chart 1), in which two incomplete cuboidal subunits, $M_4(\mu_3\text{-S})_3$ ($M = \text{Ru}, \text{Mo}, \text{and Cu}$), are linked by two $\mu_2\text{-I}$ bridges. Although both Cu1 and Cu2 have a trigonal planar coordination geometry, Cu2 has an interaction with the neighboring $\text{I}2^*$ atom to reflect a dimerization in cluster **4** {the distances of Cu2–I2 and Cu2–I2* are 2.514(2) and 2.972(2) Å, respectively}. Such an octanuclear framework with the weak bridging I interactions has also been observed in $[\text{NEt}_4]_4[\text{Cu}_6\text{Mo}_2\text{S}_6\text{O}_2\text{I}_6]$ {the distances of Cu–I are 2.517(2) and 2.984(3) Å} and $[\text{NEt}_4]_4[\text{Cu}_6\text{Mo}_2\text{S}_6\text{O}_2\text{Br}_2\text{I}_4]$ {the distances of Cu–I are 2.502(2) and 2.972(3) Å} previously determined by X-ray analysis.⁴⁷ The Mo atom has a distorted tetrahedral coordination geometry with one Mo–O bond {1.693(7) Å} and three Mo–($\mu_3\text{-S}$) bonds (approximately same as one another: av. 2.273 Å) reflecting one strong $\nu_{\text{Mo-S}}$ band at 445 cm^{-1} of an IR spectrum as a KBr disk of **4**.

Synthesis and Structure of $[\text{Ru}(\eta^6\text{-C}_6\text{Me}_6)\{\text{P}(\text{OMe})_3\}\{\text{MoO}(\mu_3\text{-S})_3\}(\text{CuI})_2\}$ (5** without an Inversion Center).** Red

crystals used in the X-ray analysis of **5** were obtained from a DMF solution of the mixture of **4** and **5**. As depicted in Figure 5, cluster **5** has an open capsule-type octanuclear framework (type **M** in Chart 2), in which two incomplete cubane units, $M_4(\mu_3\text{-S})_3$ ($M = \text{Ru}, \text{Mo}, \text{and Cu}$), are linked by two $\mu_2\text{-I}$ bridges. To the best of our knowledge, this is the first example of such an open capsule-type cluster without an intramolecular inversion center. The Ru atom is octahedrally coordinated, and the Mo atom has a distorted tetrahedral coordination with one terminal O and three $\mu_3\text{-S}$ atoms. The Cu1 and Cu2 have a trigonal planar geometry with two S and one Cl atoms, but Cu2 has a weak interaction with the neighboring $\text{I}2^*$ atom {the distances of Cu2–I2 and Cu2–I2* are 2.497(1) and 3.046(1) Å, respectively}.

ESI-MS has rapidly been becoming one technique to probe the structure of metal complexes in solution.⁴⁸ On the basis of our background of ESI-MS studies,^{26a,48b} we have used ESI-MS to probe the structure of **5** and **6** in solution. The positive ion mass spectrum of the same crystal used in the X-ray analysis of **5** in CH_3CN shows signals at m/z 1826.4 {relative intensity (I) = 30% in the range of m/z 1300 to 2000}, m/z 1636.4 (I = 100%), and m/z 1445.4 (I = 70%) (Figure 6a). The envelope at m/z 1826.4 has a characteristic distribution of isotopomers that matches well with the calculated isotopic distribution for $[\mathbf{5} - \text{I}]^+$ (Figure 6b and 6c). In the spectrum each envelope gives a

(47) (a) Hou, H.; Long, D.; Xin, X.; Huang, X.; Kang, B.; Ge, P.; Ji, W.; Shi, S. *Inorg. Chem.* **1996**, *35*, 5363–5367. (b) Hou, H.-W.; Xin, X.-Q.; Liu, J.; Chen, M.-Q.; Shu, S. *J. Chem. Soc., Dalton Trans.* **1994**, 3211–3214.

(48) (a) Chen, P. *Angew. Chem., Int. Ed.* **2003**, *42*, 2832–2847. (b) Ogo, S.; Makihara, N.; Watanabe, Y. *Organometallics* **1999**, *18*, 5470–5474.

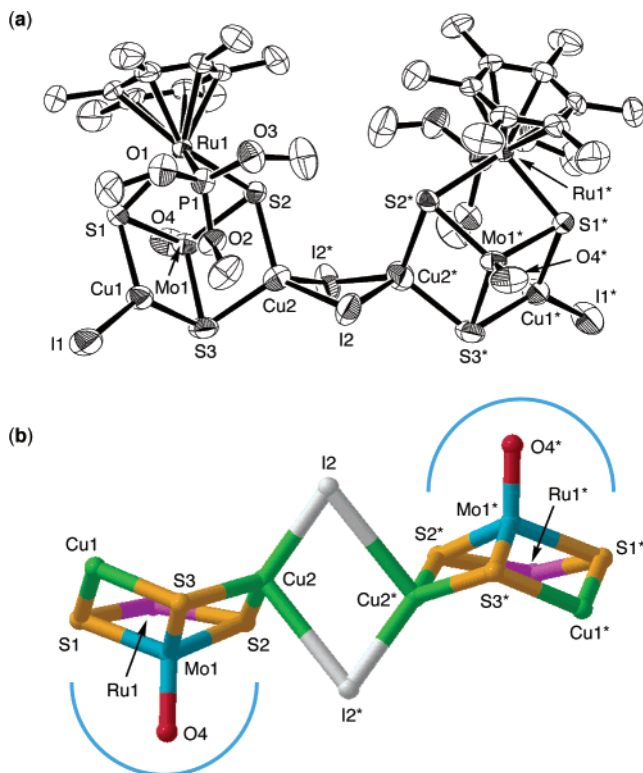


Figure 5. (a) ORTEP drawing of **5**. Selected interatomic distances (\AA) and angles (ϕ/deg): Ru1–Mo1 = 2.8979(7), Mo1–Cu1 = 2.665(1), Mo1–Cu2 = 2.674(1), Ru1–S1 = 2.381(2), Ru1–S2 = 2.388(2), Mo1–S1 = 2.275(2), Mo1–S2 = 2.281(2), Mo1–S3 = 2.272(2), Mo1–O4 = 1.694(4), Cu1–I1 = 2.450(1), Cu2–I2 = 2.497(1), Cu2–I2* = 3.046(1), Ru1–S1–Mo1 = 76.95(5), Ru1–S2–Mo1 = 76.69(5), Ru1–S1–Cu1 = 117.85(7), Ru1–S2–Cu2 = 124.00(7), S1–Mo1–O4 = 110.9(2), S2–Mo1–O4 = 114.0(2), S3–Mo1–O4 = 111.3(2), Mo1–S1–Cu1 = 71.86(5), Mo1–S2–Cu2 = 71.49(5), S1–Cu1–S3 = 108.62(7), S2–Cu2–S3 = 107.49(7), I2–Cu2–I2* = 103.49(4). (b) The open capsule-type linked incomplete double cubane framework of **5** $\{\text{C}_6\text{Me}_6, \text{P}(\text{OMe})_3\}$, and the terminal iodide ligands (I1 and I1*) are omitted for clarity.

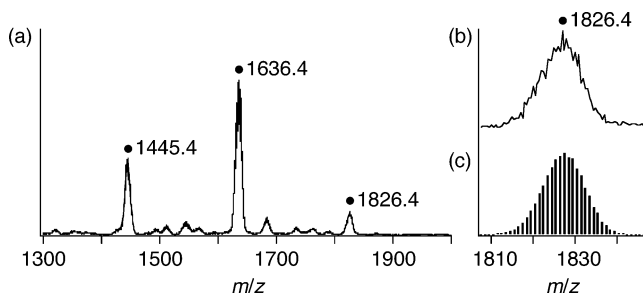


Figure 6. (a) Positive-ion ESI mass spectrum of **5** in CH_3CN . The signal at m/z 1826.4 corresponds to $[\mathbf{5} - \text{I}]^+$. The signals at m/z 1636.4 ($[\mathbf{5} - \text{I} - \text{CuI}]^+$) and 1445.4 ($[\mathbf{5} - \text{I} - 2\text{CuI}]^+$) are product ions of $[\mathbf{5} - \text{I}]^+$. (b) The signal at m/z 1826.4. (c) Calculated isotopic distribution for $[\mathbf{5} - \text{I}]^+$.

wide distribution of isotopomers due to isotopes of Mo (^{95}Mo , 15.9%; ^{96}Mo , 16.7%; and ^{98}Mo , 24.1%) and Cu (^{63}Cu , 69.2% and ^{65}Cu , 30.8%). MS/MS measurements indicate that the signals at m/z 1636.4 ($[\mathbf{5} - \text{I} - \text{CuI}]^+$) and 1445.4 ($[\mathbf{5} - \text{I} - 2\text{CuI}]^+$) are product ions of $[\mathbf{5} - \text{I}]^+$. The IR spectrum as a KBr disk of **5** exhibits the $\nu_{\text{Mo-S}}$ and $\nu_{\text{Mo-O}}$ bands at 442 and 926 cm^{-1} , respectively.

Synthesis and Structure of $[\text{Ru}(\eta^6\text{-C}_6\text{Me}_6)\{\text{P}(\text{OEt})_3\}_3\{\text{MoO}(\mu_3\text{-S})_3\}(\text{CuI})_2]$ (6**).** An incomplete single cubane-type tetranuclear sulfide cluster **6** (type **H** in Chart 1) was prepared from a reaction of butterfly-type trinuclear sulfide cluster **3b**

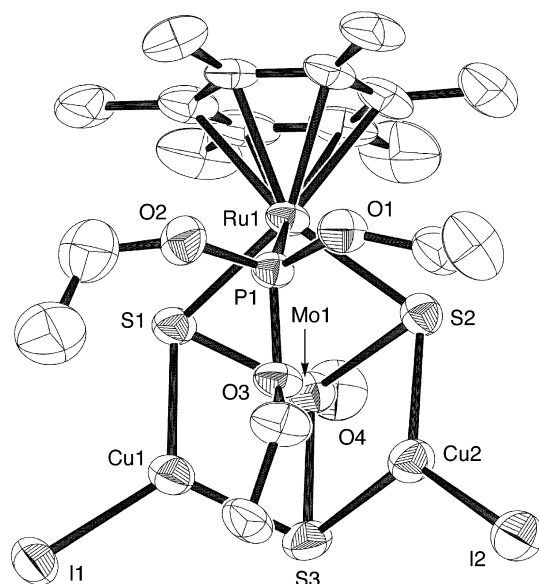


Figure 7. ORTEP drawing of **6**. Selected interatomic distances (\AA) and angles (ϕ/deg): Ru1–Mo1 = 2.878(1), Mo1–Cu1 = 2.669(1), Mo1–Cu2 = 2.655(1), Ru1–S1 = 2.390(2), Ru1–S2 = 2.385(2), Mo1–S1 = 2.279(2), Mo1–S2 = 2.277(2), Mo1–S3 = 2.270(2), Mo1–O4 = 1.716(5), Cu1–I1 = 2.452(1), Cu2–I2 = 2.452(1), Ru1–S1–Mo1 = 76.07(6), Ru1–S2–Mo1 = 76.21(6), Ru1–S1–Cu1 = 121.99(7), Ru1–S2–Cu2 = 117.41(8), S1–Mo1–O4 = 114.7(2), S2–Mo1–O4 = 110.7(2), S3–Mo1–O4 = 111.1(2), Mo1–S1–Cu1 = 72.13(6), Mo1–S2–Cu2 = 71.43(6), S1–Cu1–S3 = 108.62(8), S2–Cu2–S3 = 108.69(7).

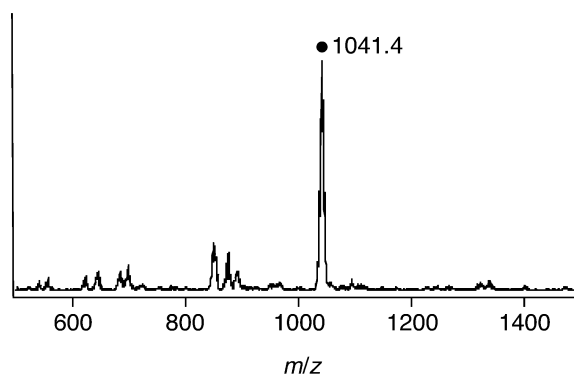


Figure 8. Positive-ion ESI mass spectrum of **6** in CH_3CN . The signal at m/z 1041.4 corresponds to $[\mathbf{6} + \text{Na}]^+$.

with an equimolar CuI. Red crystals of **6** used in the X-ray analysis (Figure 7) were obtained from a DMF/diethyl ether solution of **6**. Figure 7 shows that a very bulky ligand of triethyl phosphite prevents dimerization of **6**. Thus, the IR spectrum of **6** measured in DMF exhibits one $\nu_{\text{Mo-S}}$ band (442 cm^{-1}) and one $\nu_{\text{Mo-O}}$ band (927 cm^{-1}); these values agree well with those obtained in the solid state (as a KBr disk) at 442 cm^{-1} ($\nu_{\text{Mo-S}}$) and 927 cm^{-1} ($\nu_{\text{Mo-O}}$).

The positive ion ESI mass spectrum of **6** in CH_3CN in Figure 8 shows a prominent signal at m/z 1041.4 ($I = 100\%$ in the range of m/z 500 to 1500), which corresponds to $[\mathbf{6} + \text{Na}]^+$.

Thermal Stability of $[\text{Ru}(\eta^6\text{-C}_6\text{Me}_6)\{\text{P}(\text{OMe})_3\}_3\{\text{MoO}(\mu_3\text{-S})_3\}(\text{CuI})_2]$ (5**) and $[\text{Ru}(\eta^6\text{-C}_6\text{Me}_6)\{\text{P}(\text{OEt})_3\}_3\{\text{MoO}(\mu_3\text{-S})_3\}(\text{CuI})_2]$ (**6**).** We have performed ^1H NMR measurements of **5** and **6** dissolved in acetonitrile in order to compare the thermal stability in solution. Figure 9a–c show the time-dependent C_6Me_6 signals in ^1H NMR spectra of **5** in CD_3CN , indicating that the structure of the octanuclear cluster **5** is preserved in

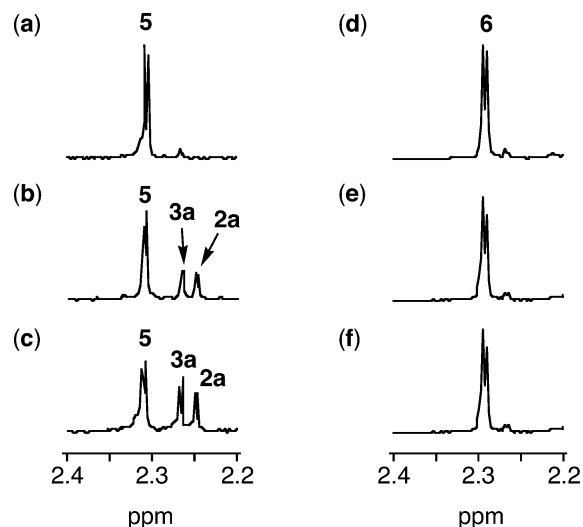


Figure 9. Time-dependent C_6Me_6 signals in 1H NMR spectra of **5** in CH_3CN for 1 h (a), 24 h (b), and 36 h (c). Time-dependent 1H NMR spectra of **6** in CH_3CN for 1 h (d), 24 h (e), and 36 h (f).

CH_3CN for 1 h but that it slowly decomposes to the trinuclear cluster **3a** and the dinuclear cluster **2a**.⁴⁹ On the other hand, the structure of tetranuclear cluster **6** is stable for 36 h in acetonitrile (Figure 9d–f). Thus, the thermal stability of the octanuclear cluster **5** dissolved in solution is quite different from that of the tetranuclear cluster **6** in the same solvent.

Methodology for the Building Block Construction of Heterometallic Sulfide Clusters. The successful methodology for the building block construction of heterometallic sulfide clusters in this study is summarized in Scheme 2 as polyhedron figures of **1a**, **1b**, **2a**, **2b**, **3a**, **3b**, **4**, **5**, and **6**. The butterfly-type trinuclear sulfide clusters **3a** and **3b** as key precursors for the synthesis of **4**, **5**, and **6** were prepared stepwise in methanol and acetonitrile from the mononuclear building blocks with different coordination abilities (vide infra). The mononuclear ruthenium complexes **1a** and **1b** have been used as a starting material in which **1a** and **1b** with bulky C_6Me_6 and $P(OR)_3$ ligands are employed as an octahedral terminal building block

(49) The C_6Me_6 signals due to the corresponding tetranuclear cluster cannot be distinguished from those of the octanuclear cluster **5** because of the weak bridging interaction as indicated by the X-ray structure of **5** in Figure 5. Although the ESI mass spectrum of **5** in Figure 6 clearly indicates the existence of the octanuclear cluster **5** in solution, the coexistence of the corresponding tetranuclear cluster in solution cannot be ruled out.

to control the direction of the cluster expansion. The Cl ligands of **1a** and **1b** are readily replaced by the S atoms of $[MoOS_3]^{2-}$, which functions as a tetrahedral polydentate building block owing to the strong coordination ability of the S atoms. The dinuclear complexes **2a** and **2b** were generated from a reaction of **1a** and **1b** with $[MoOS_3]^{2-}$. The CuI building block binds to the S atoms of $[MoOS_3]^{2-}$ to form a trigonal planar $(\mu-S)_2CuI$ unit of the butterfly-type trinuclear sulfide clusters **3a** and **3b**.

In the case of trimethyl phosphite $\{P(OMe)_3\}$ used as a supporting ligand of the ruthenium complex, octanuclear incomplete double cubane clusters **4** and **5** were generated by a reaction of the butterfly-type trinuclear sulfide clusters **3a** with the CuI building block. When trimethyl phosphite $\{P(OMe)_3\}$ was replaced by triethyl phosphite $\{P(OEt)_3\}$ as a supporting ligand of the ruthenium complex, however, only the tetranuclear incomplete single cubane-type cluster **6** was generated due to the steric effect of the triethyl phosphite $\{P(OEt)_3\}$ group, which is more bulky than trimethyl phosphite $\{P(OMe)_3\}$. This indicates that open capsule-type octanuclear sulfide clusters **5** and **6** are attained by controlling the bulkiness of a supporting ligand.

Conclusions

A building block approach in Schemes 1 and 2 has been successfully employed to stepwise construct the target cluster **5**, which is an open capsule-type octanuclear heterometallic sulfide cluster with the linked incomplete double cubane framework without an intramolecular inversion center. Such a building block approach provides a valuable strategy in developing new structural models for the defective surface of heterogeneous sulfide or oxide catalysts and for the molecular recognition sites in enzymes with cubane-type units.

Acknowledgment. This work was supported by a grant in aids (15036242, 15350033, 16205020, and 16655022) from the Ministry of Education, Culture, Sports, Science, and Technology, Japan, Osaka University 21st Century COE Program, and a CREST program (Nano-Structured Catalysts and Materials) by JST. We thank emeritus Professor M. Misono (University of Tokyo) for valuable discussions.

Supporting Information Available: Crystallographic data (CIF) for **1a**, **2a**, **3a**, **3b**, **4**, **5**, and **6**. This material is available free of charge via the Internet at <http://pubs.acs.org>.

JA051748Q